A EUROPEAN JOURNAL OF CHEMICAL BIOLOGY

CHEMBIOCHEM

SYNTHETIC BIOLOGY & BIO-NANOTECHNOLOGY

Accepted Article

Title: Photopharmacological Control of Cyclic Antimicrobial Peptides

Authors: Andrew David Abell, Jingxian Yu, Steven Polyak, John Horsley, and Yuan Qi Yeoh

To be cited as: *ChemBioChem* 10.1002/cbic.201800618

Link to VoR: http://dx.doi.org/10.1002/cbic.201800618

A Journal of ChemPubSoc Europe

WILEY-VCH www.chembiochem.org

WILEY-VCH

FULL PAPER

Photopharmacological Control of Cyclic Antimicrobial Peptides

Yuan Qi Yeoh,[a] Jingxian Yu,[a] Steven W. Polyak,[b] John R. Horsley,[a] Andrew D. Abell*[a]

Abstract: Gramicidin S is a naturally occurring antimicrobial cyclic peptide. Here we present a series of cyclic peptides based on Gramicidin S each containing an azobenzene photoswitch to reversibly control secondary structure and, hence, antimicrobial activity. ^{1}H NMR and density functional theory (DFT) calculations revealed a β-sheet/β-turn secondary structure for the *cis* configuration of each peptide, and an ill-defined conformation for all associated *trans* structures. The *cis*-enriched and *trans*-enriched photostationary states (PSS) for each of peptides **1**-**3** were assayed against *Staphylococcus aureus* (*S. aureus*) to reveal a clear relationship between well-defined secondary structure, amphiphilicity and optimal antimicrobial activity. Most notably, peptides **2a** and **2b** exhibited a four-fold difference in antimicrobial activity in the *cis*-enriched PSS over the *trans*-enriched equivalent. This photopharmacological approach allows antimicrobial activity to be regulated through photochemical control of the azobenzene photoswitch, opening new avenues in the design and synthesis of future antibiotics.

Introduction

Gramicidin S (Figure 1) is a naturally occurring cyclic peptide-based antibiotic with a symmetrical antiparallel β-sheet conformation, linked by two type-II' β-turns.[1] The antimicrobial properties of Gramicidin S have been attributed to its well-defined β-sheet secondary structure, and overall amphiphilic character.[2] The peptide contains two basic ornithine amino acids and a series of hydrophobic amino acids, allowing Gramicidin S to bind to and penetrate anionic microbial lipid membranes.[3] Gramicidin S is particularly active against Gram positive *S. aureus*,[4] making it a potentially potent antibiotic to treat a range of specific bacterial infections. Photopharmacology presents as an ideal approach to regulate the activity of Gramicidin S to allow further exploitation of its desirable antimicrobial properties. Specifically, the introduction of a photoswitch into its backbone allows reversible control of the secondary structure and, hence, binding affinity, aggregation, and folding properties.[5] Antimicrobial activity can then be switched 'on' or 'off' upon irradiation with light of a specific wavelength, with spatiotemporal precision. This would enhance selectivity and likely reduce toxicity and potential for the development of antimicrobial resistance.[6] Previous studies have illustrated the role of a photoswitch in such a photopharmacological approach to modulate the activity of membrane channels,[7] enzyme inhibitors,[8] anticancer drugs,[9] and other antibiotics.[10] A recent study incorporated a diarylethene photoswitch into the backbone of Gramicidin S to regulate antimicrobial activity.[11]

Herein, a series of photoswitchable antimicrobial peptides (**1**-**3**, Figure 1) based upon Gramicidin S was synthesized for an extended study, each containing a meta/para-substituted azobenzene photoswitch incorporated into its backbone. These peptides were chosen to define the role of secondary structure and amphiphilicity on antimicrobial activity, with both *cis*-enriched and *trans*-enriched PSS assayed against *S. aureus*. An azobenzene was chosen for incorporation into the peptide backbone of Gramicidin S as it is known to give rise to a significant geometric change, high photoisomerization yield and fast isomerization, while having a relative ease of synthesis.[12] In addition, an azobenzene in its *cis* conformation is known to mimic the β-turn in β-hairpin structures.[13] We anticipated that a suitable azobenzene in its *cis* conformation would mimic the β-turn of the native Gramicidin S, allowing the peptide to adopt a β-sheet structure. This Gramicidin S mimetic would be expected to be active in suppressing microbial growth, whereas the corresponding *trans* isomer with its ill-defined random structure, would not.

Results and Discussion

Design and Synthesis of Peptides 1-3

Cyclic peptides **1**-**3** (Figure 1) mimic the structure and conformation of natural Gramicidin S, which has the amino acid sequence, cyclo(^{D}FPVOL^{D}FPVOL) (^{D}F=D-phenylalanine, O=ornithine). Peptide **1** has a similar amino acid sequence to Gramicidin S, with proline and D-phenylalanine residues replaced by the azobenzene photoswitch. Proline and D-phenylalanine were positioned in the β-turn region of the native Gramicidin S, where these residues are known to generate a well-defined turn in a cyclic structure.[11, 14] A meta/para-substituted azobenzene photoswitch (red highlighted region in peptides **1**-**3**, Figure 1) was chosen because of its propensity to mimic the desired β-turn as defined by modelling discussed below. The remaining amino acid residues native to Gramicidin S were retained in peptide **1**, so as to maintain the amphiphilic side chain pattern required for biological activity.[2d] It was anticipated that, by mimicking the β-turn found in the native Gramicidin S, the *cis* isomer of the azobenzene photoswitch would bring both β-strands into close proximity to preserve the well-defined secondary structure of the peptide. Thus, *cis*-peptide **1** was expected to retain antimicrobial activity. Conversely, the azobenzene photoswitch in its *trans*

[a] *Y. Q. Yeoh, Dr. J. Yu, Dr. J. R. Horsley, Prof. A. D. Abell*
ARC Centre of Excellence for Nanoscale BioPhotonics (CNBP)
Department of Chemistry
The University of Adelaide, SA 5005, Australia.
Email: andrew.abell@adelaide.edu.au

[b] *Dr. S. W. Polyak*
School of Biological Sciences
Department of Molecular and Cellular Biology
The University of Adelaide, SA 5005, Australia.

Supporting information for this article can be found under: http://dx.doi.org/10.1002/chem.2018xxxxx.

10.1002/cbic.201800618

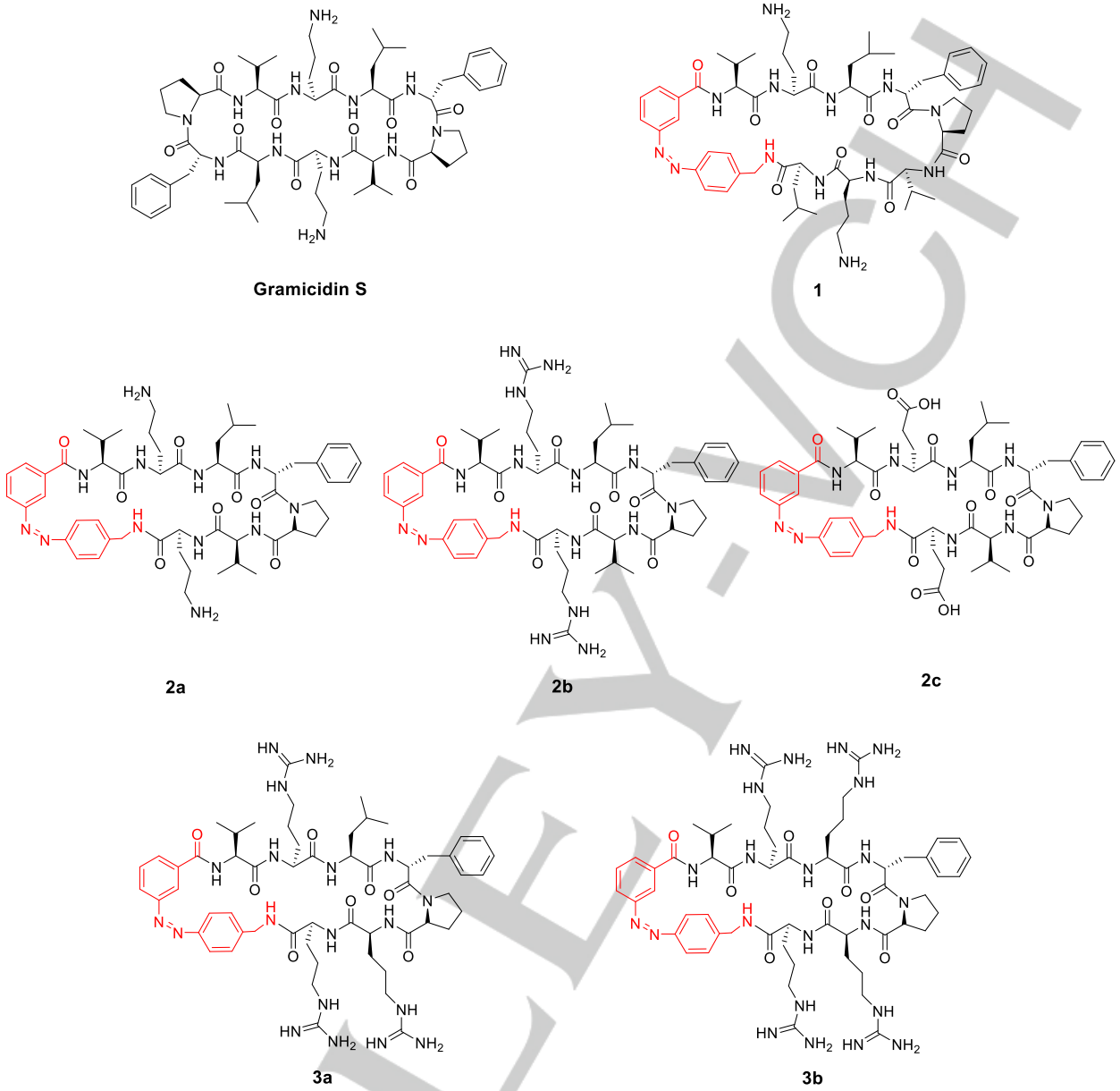

Figure 1. Structure of Gramicidin S and its mimetics, peptides **1-3** (*cis* isomers). The azobenzene photoswitch is highlighted in red in peptides **1-3**.

configuration would be expected to disrupt the β-sheet/β-turn character of peptide **1** and, hence, result in diminished activity. Modelling of *cis*-peptide **1** by DFT calculations revealed a distortion in its β-strand secondary structure due to strain exerted by the photoswitch on the peptide backbone (see Figure S3). The leucine residue was removed from the underside strand of **1** to give peptide **2a** in order to further explore this supposition. Ensuing computational data on **2a** was consistent with a more well-defined β-strand secondary structure. An alternative basic amino acid residue (arginine) and an acidic amino acid residue (glutamic acid) were incorporated into the structure to investigate the effect of positive and negative charges on antimicrobial activity, as in peptides **2b** and **2c** respectively. Hence, any observed differences in antimicrobial activity would then be directly attributable to the positively or negatively charged amino acid residues, as the active *cis* isomers of **2a-2c** would be expected to adopt similar secondary structures. The role of amphiphilicity on antimicrobial activity was investigated by incorporating additional basic amino acids residues into the peptide backbone (**3a** and **3b**) in place of the hydrophobic amino acids leucine and valine.

All peptides and a Gramicidn S control were synthesized by solid phase peptide synthesis (SPPS) as outlined in the Experimental section, and crude products purified by RP-HPLC prior to biological testing. The component azobenzene photoswitch was synthesized using an existing methodology.[15]

Spectroscopic Analysis for Peptides 1-3

For all experiments, the thermally stable *trans*-enriched PSS was isomerized to a *cis*-enriched PSS by irradiation using UV light (352 nm). Conversely, *cis* to *trans* isomerism was induced by irradiation with visible light (405 nm). The *trans*-enriched PSS of each peptide (**1**-**3**) exhibited a broad absorption band (λ_{max} = 328-330 nm, Table 1, Figure S1) whereas each *cis*-enriched PSS displayed a stronger absorbance at 428 nm, and an absorbance of much lower intensity at 328-330 nm. These observed values concur with literature.[16] The intense absorbance at 328-330 nm is due to the symmetry allowed $\pi \rightarrow \pi^*$ transition, while the weak absorbance peak at 428 nm is the result of the symmetry forbidden $n \rightarrow \pi^*$ transition.[17] A far less intense absorption band at 328 nm was apparent for the *cis*-enriched PSS of peptides **1**-**3**, which is likely due to a small amount of *trans* isomer remaining after irradiation. Both azobenzene isomers are known to give some overlap of absorption spectra.[18] A more quantitative measure of each photostationary state was determined by the ratio of ^{1}H NMR intergrals at δ 7.83 ppm and δ 6.81 ppm (see Supporting Data). These ^{1}H NMR resonances correspond to hydrogens of the *para*-substituted phenyl ring in the *trans* and *cis* isomers of the azobenzene unit respectively.[19] It was determined that the photoisomerization yield for the *cis*-enriched PSS of peptides **1**-**3** was relatively high, ranging from 64%-90% as detailed in Table 1. The secondary structures of the peptides **1**-**3** were defined by ^{1}H NMR, with $^3J_{NHC\alpha H}$ coupling constants in the range of 8-10 Hz[20] for a β-strand. Analysis of the *cis*-enriched PSS of **2a**-**2c** revealed $^3J_{NHC\alpha H}$ coupling constants of 8.0-8.8 Hz, consistent with a more well-defined β-strand structure than the *cis* isomers of **1** and **3**. The half-lives for the *cis*-enriched PSS of each peptide (Table 1, Figure S2) were determined to be between 2-4 days, by analyzing the kinetics of the *cis*-*trans* thermal back isomerization. However, the *cis*-enriched PSS of peptides **2a**-**2c** have longer half-lives than the *cis*-enriched PSS of peptides **1** and **3**, which have less well-defined secondary structures as revealed by ^{1}H NMR. The half-lives for the *cis*-enriched PSS of peptides **2a**-**2c** range between 3.5-4 days, thus highlighting their robustness and stability. This considerable time frame is sufficient for antimicrobial assaying against *S. aureus*, which in this case was 16-20 hours.

Molecular Modelling for Peptides 1-3

The lowest energy conformer for the *cis* isomer of peptide **1** was determined by density functional theory (DFT). The resulting model revealed four intramolecular hydrogen bonds linking the upper and lower strands, with two of these considered strong bonds (2.0 Å and 2.2 Å), and the other two moderate to weak (2.5 Å and 3.8 Å). The *cis* isomers of peptides **2** and **3** contain three strong hydrogen bonds (1.8 Å-2.0 Å, Table S3). In comparison, native Gramicidin S possesses four strong intramolecular hydrogen bonds (2.0 Å-2.2 Å) connecting the upper and lower strands of the cyclic peptide, which play an important role in defining its β-sheet structure. The *trans* isomers for each of peptides **1**-**3** lack intramolecular hydrogen bonding and, hence, secondary structure. The computational molecular models for both isomers of **2b** are shown in Figure 2 to highlight this structural disparity. The calculated backbone dihedral angles (Table S4) for the *trans* isomers of peptides **1**-**3** were found to be outside the allowable ϕ, ψ and ω angles specific to a β-strand structure.[21] A standard β-sheet should contain more than 30% β-sheet content.[22] The *cis* isomers of peptides **2a**-**2c** were found to contain 43 % β-sheet content, while the *cis* isomers of peptides **1** and **3** contain 29 % (see Table S4). Notably, the *cis* isomer of **1** showed a large kink on the underside of the backbone which distorts the β-sheet structure of the peptide as shown in Figure S3. A β-turn is denoted by four consecutive 'corner' amino acid residues *i* to *i*+3,[14] and is considered to be present if two specific criteria are fulfilled: i) a distance of less than 7 Å between the C_α (*i*) and C_α (*i*+3), and ii) the (*i*+1) and (*i*+2) residues are not in an α-helix.[23] Based on these parameters, the *cis* isomer of peptides **1**-**3** contains a β-turn, with C_α (*i*) to C_α (*i*+3) distances ranging between 5.7 Å and 6.0 Å (Table S3). The corresponding distance for each of the *trans* isomers of **1**-**3** exceeds 7 Å, indicative of the random nature in each case.

Biological Assay for Peptides 1-3

Peptides **1**-**3** and Gramicidin S were assayed for their antibacterial activity against *S. aureus* ATCC 49775, as detailed in the Experimental section. The minimum inhibitory concentration (MIC) of the prototypical peptide Gramcidin S was in agreement with prevous reports[11, 24] (2 μg/mL, Table 2). No detectable difference in bioactivity was observed between the *cis*-enriched and *trans*-enriched PSS of **1** (MIC 64 μg/mL). This result is consistent with the earlier molecular modelling study which showed a distorted β-strand secondary structure in peptide **1** due to the photoswitch. Peptides **2a** and **2b**, both designed to address the strain on the peptide backbone, showed differential bioactivity due to photoswitching. For **2a**, the *cis*-enriched PSS was four-fold more active than the *trans*-enriched equivalent (Table 2). This important finding demonstrates that the antimicrobial activity of the peptide can be regulated by controlling the peptide secondary structure through photoisomerization. Consistent with this observation, the *cis*-enriched PSS of **2b** also afforded four-fold greater bioactivity over its *trans*-enriched equivalent. Indeed, *cis*-enriched **2b** provided the most potent antibacterial analogue in this series (MIC 32 μg/mL). These findings are consistent with our design principles where substitution of ornithine residues with arginine residues, as in peptide **2b**, was predicted to enhance membrane penetrating properties,[25] resulting in improved

Table 1. Photoisomerization yields and half-lives of Gramicidin S mimetics, peptides **1**-**3**, in their respective photostationary states.

Peptide	**1**		**2a**		**2b**		**2c**		**3a**		**3b**	
Photostationary State (PSS)	*cis*	*trans*	*cis*	*trans*	*cis*	*trans*	*cis*	*trans*	*cis*	*trans*	*cis*	*trans*
Photoisomerization Yield (%)	90	84	90	88	71	75	90	85	84	66	64	67
Half-Life (min)	4489	-	5051	-	5996	-	5819	-	5269	-	2901	-

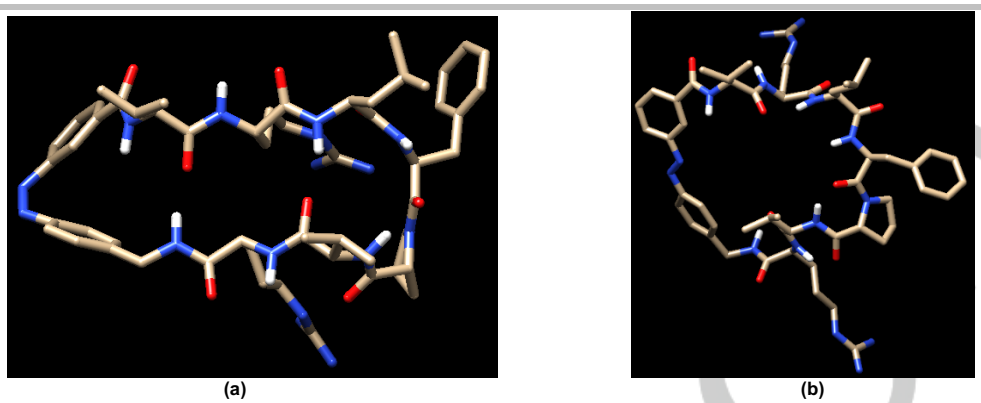

(a) (b)

Figure 2. Molecular models of peptide **2b (a)** *cis* isomer and **(b)** *trans* isomer, showing the large disparity between the two structures.

Table 2. Minimum inhibitory concentration (MIC) of Gramicidin S and its mimetics, peptides **1**-**3**, in their respective photostationary states.

Peptide	Gramicidin S	**1**		**2a**		**2b**		**2c**		**3a**		**3b**	
Photostationary State (PSS)	-	*cis*	*trans*	*cis*	*trans*	*cis*	*trans*	*cis*	*trans*	*cis*	*trans*	*cis*	*trans*
Minimum Inhibitory Concentration (MIC) (μg/mL)	2	64	64	64	256	32	128	>256	>256	256	>256	>256	>256

antimicrobial activity. In further agreement, both PSS of the glutamic acid-containing peptide **2c** were inactive against *S. aureus* at the highest concentration tested (256 μg/mL), confirming the importance of basic amino acids for antimicrobial activity. Replacement of hydrophobic residues valine and leucine with arginine residues (**3a** and **3b**) resulted in a decrease in antimicrobial activity, presumably due to disruption of the amphiphilic nature of the peptides with associated decreased penetration through the bacterial membrane. As **3a** and **3b** both possess approximately 30% β-sheet character (see Table S4), we postulate that amphiphilicity plays a more significant role than secondary structure in this context. Together, our experimental and computational data shows that antimicrobial activity in these Gramicidin S peptide mimetics is dependent on a fine balance between well-defined secondary structure and the amphiphilic nature of the amino acid side chains. Indeed, our Gramicidin S analogues have indicated a synergy between these two factors, where the well-defined β-sheet framework is likely essential for stabilizing the residues responsible for maintaining amphiphilicity.

Conclusions

In this study, a series of photoswitchable cyclic peptides (**1**-**3**) based on the antimicrobial agent Gramicidin S was synthesized, each containing an azobenzene moiety for reversible switching between a *trans* isomer possessing an ill-defined conformation, and a *cis* isomer containing a well-defined secondary structure. Each peptide was assayed against *S. aureus*, with photoisomerization from *trans*-enriched to *cis*-enriched PSS resulting in significant differences in biological activity. Specifically, peptides **2a** and **2b** showed a four-fold difference in the minimum inhibitory concentration (MIC) values against *S. aureus*, between their respective *cis*-enriched and *trans*-enriched PSS, with the well-defined *cis*-enriched PSS found to be more active. These results confirmed that the secondary structure of the peptide and, hence, antimicrobial activity can be regulated through photochemical control of the azobenzene photoswitch. Replacement of the hydrophobic valine and leucine residues with basic arginine residues gave peptides **3a** and **3b**, which were devoid of activity. Collectively, these results show that both well-defined secondary structure and amphiphilicity are essential for antimicrobial activity against *S. aureus*. Furthermore, our findings suggest it is possible that amphiphilicity is more important for membrane penetration, where no conformational molecular recognition is required, unlike for most protein-protein interactions for example, where well-defined secondary structure is crucial. This photopharmacological approach may offer benefits for the design of future antibiotics that possess significant therapeutic value, but are limited by factors such as bioavailability. This important strategy provides an opportunity to turn antimicrobial activity 'on' and 'off' to allow potential future point-of-care applications.

Experimental Section

Detailed characterization of Gramicidin S and peptides **1**-**3** are provided in the Supporting Data.

Synthesis of Azobenzene Photoswitch

3-nitrosobenzoic acid: To a solution of 3-aminobenzoic acid (5.0 g, 36.5 mmol) in dichloromethane (100 mL), a solution of oxone (22.4 g, 73.0 mmol) in water (400 mL) was added dropwise, and the mixture was stirred vigorously for 4 h at rt. The mixture was filtered and dried overnight under vacuum to yield a yellow solid (5.0 g, 90%). ^{1}H NMR (500 MHz, DMSO-d_6): δ 8.41-8.39 (m, 1H), 8.36-8.35 (m, 1H), 8.20-8.17 (m, 1H), 7.89 (t, J = 7.8 Hz, 1H).

(9*H*-fluoren-9-yl) methyl 4-aminobenzylcarbamate: To a mixture of 4-aminobenzylamine (2.0 g, 16.4 mmol) in water (32 mL) and tetrahydrofuran (12 mL), 5% $NaHCO_3$ (1.5 mL) was added, and the mixture was stirred for 10 min at rt. *N*-(9-fluorenylmethoxycarbonyloxy)succinimide (5.5 g, 16.4 mmol) was suspended in tetrahydrofuran (20 mL) and the suspension was added dropwise, and the mixture stirred for 24 h at rt. Water (500 mL) was added to the mixture and the product was precipitated as a pale yellow solid. The precipitate was filtered and dried *in vacuo* to give a yellow solid (4.8 g, 84%). ^{1}H NMR (500 MHz, DMSO-d_6): δ 7.88 (d, *J* = 7.5 Hz, 1H), 7.69 (d, *J* = 7.5 Hz, 1H), 7.63 (t, *J* = 6.0 Hz, 1H), 7.41 (t, *J* = 7.3 Hz, 1H), 7.32 (t, *J* = 7.5 Hz, 1H), 6.88 (d, *J* = 8.2 Hz, 1H), 6.49 (d, *J* = 8.3 Hz, 1H), 4.30 (d, *J* = 7.0 Hz, 1H), 4.21 (d, *J* = 6.7 Hz, 1H), 3.99 (d, *J* = 6.0 Hz, 1H).

Azobenzene Photoswitch: To a solution of 3-nitrosobenzoic acid (2.3 g, 15.4 mmol) in DMSO (50 mL), glacial acetic acid (50 mL) was added, and the mixture was stirred for 10 min at rt. (9*H*-fluoren-9-yl) methyl 4-aminobenzylcarbamate (2.6 g, 7.7 mmol) was added to the reaction mixture and stirred overnight under N_2 at rt. The mixture was filtered under suction to reveal an orange solid. The remaining product in the filtrate was extracted by DCM (50 mL), and the mixture was washed with water (2 x 50 mL) to remove acetic acid/DMSO. The organic layer was removed under N_2 to obtain an orange solid. The two orange solids were combined and dried *in vacuo*. The crude product was purified by column chromatography (9:1 DCM/methanol) to give an orange solid (2.3 g, 63%). R.f (9:1 DCM/methanol) = 0.4. ^{1}H NMR (500 MHz, DMSO-d_6): δ 13.30 (s, 1H), 8.38 (s, 1H), 8.16-8.11 (m, 2H), 7.95 (t, *J* = 6.1 Hz, 1H), 7.90 (d, *J* = 6.9 Hz, 4H), 7.76-7.71 (m, 3H), 7.45-7.40 (m, 4H), 7.34 (t, *J* = 7.4 Hz, 2H), 4.40 (d, *J* = 6.7 Hz, 2H), 4.29 (d, *J* = 6.0 Hz, 2H), 4.25 (t, *J* = 6.5 Hz, 1H). HRMS (m/z): $[M+H]^+_{calc}$= 478.1722, $[M+H]^+_{found}$ = 478.1759.

Synthesis of Gramicidin S and Peptides 1-3

Synthesis of Linear Peptides by SPPS

Standard Fmoc-based SPPS and commercially available reagents were used for the synthesis of the linear peptides. Fmoc-D-Phe preloaded 2-chlorotrityl resin with a loading of 0.58 mmol/g (1.0 g, 1 equiv.) was used to synthesize the linear precursors. The unreacted active sites on the resin were capped with 17:2:1 DCM/MeOH/DIPEA (2 x 25 mL) for 30 min before washing the resin with DCM (x3), DMF (x3) and DCM (x3). *N*-Fmoc deprotection was carried out by treating the resin with 25% piperidine/DMF (25 mL) for 30 min before washing with DCM (x3), DMF (x3) followed by DCM (x3). Couplings of the amino acids and azobenzene photoswitch, were performed using the following molar ratios of reagents: Fmoc-amino acids and Fmoc-azobenzene photoswitch (2 equiv.) dissolved in DMF (20 mL), 0.5M HATU/DMF (2 equiv.) and DIPEA (8 equiv.). The resin was washed with DCM (x3), DMF (x3) followed by DCM (x3) and the coupling procedures were repeated. The coupling time in all cases was 2 h. Deprotection and coupling procedures were repeated alternatively until the sequence was completed. After the peptide sequences were completed and deprotected, the resin was washed with DCM (x3), DMF (x3) followed by DCM (x3) and dried under vacuum. The linear precursors were cleaved from the resin using 1.5% TFA in DCM (2 x 20 mL) while maintaining the side chain protection of ornithine/arginine/glutamic acid residues. The reagents were left to stand for 15 min with stirring before filtering the peptide solution. The volatile products from the filtrate were removed by N_2 flow, and the linear peptides were placed under vacuum for 4 h, to yield a crude orange solid.

Cyclization of Linear Peptides

Respective solutions of crude linear peptides in methanol (22 mg/mL) were irradiated by UV light (λ = 352 nm) for 4 h, to convert the azobenzene into its *cis* isomer prior to cyclization. The solvent was removed *in vacuo*, and the residue placed under vacuum for 30 min. The linear peptides were each dissolved in dry DMF (0.03 mmol/mL) and cyclized using the following reagents: HOBt (5 equiv.), EDC.HCl (5 equiv.) and DIPEA (10 equiv.) in dry DMF (63 mL). The mixture was kept away from visible light using an aluminium foil cover and stirred overnight under N_2 conditions at rt. DMF was then removed by N_2 flow. The crude cyclic peptides were washed with toluene (3 x 20 mL) and methanol (3 x 30 mL) to remove residual DMF and the solvent was removed *in vacuo*. The cyclic peptides were then dissolved in DCM (60 mL) and the solutions were washed with saturated $NaHCO_3$ (4 x 60 mL) and brine (2 x 60 mL). The organic layer was dried over $MgSO_4$ and the solvent removed *in vacuo*. The residue was dried under vacuum for 4 h to yield an orange solid.

Deprotection of Side Chain Protecting Groups

The Boc protecting groups on the side chains of all ornithine residues were removed by treatment with 50% TFA/DCM (10 mL) (v/v) for 60 min. The volatiles were removed by a stream of N_2 to give Gramicidin S and peptides **1** and **2a**, as orange solids. The Pbf protecting groups on the side chains of all arginine residues were removed by treatment with 95% TFA/2.5% TIPS in water (10 mL) for 60 min. The volatiles were removed by a stream of N_2 to give peptides **2b** and **3a**-**3b**, as orange solids. The tBu protecting groups on the side chains of both glutamic acid residues were removed by treatment with 90% TFA/DCM (10 mL) (v/v) for 60 min. The volatiles were removed by a stream of N_2 to give peptide **2c** as an orange solid. All crude products were purified by RP-HPLC. Fraction collection was set for peak-based collection at 220 nm and 320 nm for Gramicidin S and peptides **1**-**3** respectively. The identity of the pure products was confirmed by mass spectrometry.

Photoisomerization of Peptides 1-3

Peptides **1**-**3** were dissolved in DMSO at a concentration of 100 µg/mL and exposed to visible light of 405 nm for 2 h to yield the *trans*-enriched PSS. The *trans*-enriched PSS of **1**-**3** were irradiated by UV light of 352 nm for 2 h, to convert to the respective *cis*-enriched PSS.

Half-Life Analysis of Peptides 1-3

The half-life of peptides **1**-**3** was determined by UV-Vis spectrophotometry.[26] Prior to irradiation, peptides **1**-**3** in their thermally stable *trans*-enriched PSS, were dissolved in DMSO and the wavelengths of maximum absorbance (λ_{max}) were measured using a Synergy H4 Hybrid Multi-Mode Microplate Reader. The peptides were then irradiated under UV light (352 nm) for 2 h, to convert the samples to their *cis*-enriched PSS, and the λ_{max} were determined. The samples were irradiated under UV (352 nm) for a further 30 min to achieve the maximum attainable *cis*-enriched PSS, which was confirmed when no further increase was observed in the absorbance. Each peptide in its *cis*-enriched PSS was stored in the dark, to switch the samples back to their respective *trans*-enriched PSS by thermal relaxation. The absorbance for each peptide was measured every 10 min to monitor the change in the absorbance at 328 nm, which is characteristic of the *trans*-enriched PSS. The measurements were conducted over a period of 62 h. The absorbance at 328 nm increased gradually over 62 h for all peptides, which indicated the *cis*-*trans* thermal back isomerization. The absorbance curves at 328 nm gradually reached a plateau when the peptides reached their maximum attainable *trans*-enriched PSS. The half-life for each peptide was calculated by analyzing the increase in the UV-Vis absorbance curves[26] at 328 nm, using curve fitting in the GraphPad Prism 7.03 software.

Molecular Modelling

The lowest energy structures for the *cis* and *trans* isomers of peptides **1-3** were determined in the gas phase using the NWChem 6.6 package,[27] with tight convergence criteria using a hybrid B3LYP functional with 6-31G** basis set for all atoms. The initial geometries of peptides **1-3** were constructed through the GaussView 5.0 package by modifying the corresponding Gramicidin S unit comprised in the X-ray crystal structure (entry code 2019361, Crystallography Open Database http://www.crystallography.net), as reported.[1b] The azobenzene moiety in either *cis* or *trans* conformation was incorporated into the cyclic structure, to replace the corner residues (proline and D-phenylalanine). Conformational analysis including dihedral angles, overall molecular lengths and intramolecular hydrogen bond lengths, were conducted using the Chimera 1.11 software.[28]

Biological Assays (Antibacterial Susceptibility Evaluation)

Antibacterial activity was determined by the microdilution broth method as recommended by the CLSI (Clinical and Laboratory Standards Institute, Document M07-A8, 2009, Wayne, PA.) using cation-adjusted Mueller-Hinton broth (Trek Diagnostics Systems, U.K.). Peptides were dissolved in DMSO. Serial two-fold dilutions of each peptide were made using DMSO as the diluent. Trays were inoculated with 5 x 10^4 CFU of *Staphylococcus aureus* ATCC 49975 in a volume of 100 µL (final concentration of DMSO was 3.2% (v/v)) and incubated at 37 °C for 16-20 h. Growth of the bacterium was quantified by measuring the absorbance at 620 nm.

Acknowledgements

This work was supported by the Australian Research Council (CE140100003). We also acknowledge the Australian National Fabrication Facility for providing the analytical facilities used in this work. The computational aspects of this work were supported by an award under the National Computational Merit Allocation Scheme for JY on the National Computing Infrastructure (NCI) National Facility at the Australian National University.

Keywords: antibiotics • photoswitchable peptides • photopharmacology • *S. aureus* • secondary structure • amphiphilicity

[1] a) B. Legrand, L. Mathieu, A. Lebrun, S. Andriamanarivo, V. Lisowski, N. Masurier, S. Zirah, Y. K. Kang, J. Martinez and L. T. Maillard, *Chemistry-a European Journal* **2014**, *20*, 6713-6720; b) A. L. Llamas-Saiz, G. M. Grotenbreg, M. Overhand and M. J. van Raaij, *Acta Crystallographica Section D-Biological Crystallography* **2007**, *63*, 401-407.
[2] a) M. Jelokhani-Niaraki, R. S. Hodges, J. E. Meissner, U. E. Hassenstein and L. Wheaton, *Biophysical Journal* **2008**, *95*, 3306-3321; b) E. Kamysz, B. Mickiewicz, W. Kamysz, S. Bielinska, S. Rodziewicz-Motowidlo and J. Ciarkowski, *Journal of Peptide Science* **2011**, *17*, 211-217; c) G. Nagamurthi and S. Rambhav, *Journal of Biosciences* **1985**, *7*, 323-329; d) E. J. Prenner, M. Kiricsi, M. Jelokhani-Niaraki, R. N. Lewis, R. S. Hodges and R. N. McElhaney, *J Biol Chem* **2005**, *280*, 2002-2011; e) J. Swierstra, V. Kapoerchan, A. Knijnenburg, A. van Belkum and M. Overhand, *European Journal of Clinical Microbiology & Infectious Diseases* **2016**, *35*, 763-769; f) M. Tamaki, S. Akabori and I. Muramatsu, *International Journal of Peptide and Protein Research* **1996**, *47*, 369-375.
[3] J. A. Tennessen, *Journal of Evolutionary Biology* **2005**, *18*, 1387-1394.
[4] a) M. Kawai, H. Yamamura, R. Tanaka, H. Umemoto, C. Ohmizo, S. Higuchi and T. Katsu, *Journal of Peptide Research* **2005**, *65*, 98-104; b) T. Mogi and K. Kita, *Cellular and Molecular Life Sciences* **2009**, *66*, 3821-3826; c) M. van der Knaap, L. T. Lageveen, H. J. Busscher, R. Mars-Groenendijk, D. Noort, J. M. Otero, A. L. Llamas-Saiz, M. J. van Raaij, G. A. van der Marel, H. S. Overkleeft and M. Overhand, *Chemmedchem* **2011**, *6*, 840-847.
[5] A. Falciatore and C. Bowler, *Current Topics in Developmental Biology, Volume 68* **2005**, *68*, 317-+.
[6] M. M. Lerch, M. J. Hansen, G. M. van Dam, W. Szymanski and B. L. Feringa, *Angewandte Chemie-International Edition* **2016**, *55*, 10978-10999.
[7] a) J. Broichhagen and D. Trauner, *Current Opinion in Chemical Biology* **2014**, *21*, 121-127; b) A. Kocer, M. Walko, W. Meijberg and B. L. Feringa, *Science* **2005**, *309*, 755-758.
[8] a) C. Karlsson, M. Blom, M. Johansson, A. M. Jansson, E. Scifo, A. Karlen, T. Govender and A. Gogoll, *Organic & Biomolecular Chemistry* **2015**, *13*, 2612-2621; b) B. Reisinger, N. Kuzmanovic, P. Loffler, R. Merkl, B. Konig and R. Sterner, *Angewandte Chemie-International Edition* **2014**, *53*, 595-598; c) D. Pearson and A. D. Abell, *Chemistry-a European Journal* **2010**, *16*, 6983-6992; d) D. Pearson, N. Alexander and A. D. Abell, *Chemistry-a European Journal* **2008**, *14*, 7358-7365; e) A. J. Harvey and A. D. Abell, *Bioorganic & Medicinal Chemistry Letters* **2001**, *11*, 2441-2444; f) B. Blanco, K. A. Palasis, A. Adwal, D. F. Callen and A. D. Abell, *Bioorganic & Medicinal Chemistry* **2017**, *25*, 5050-5054.
[9] a) M. Borowiak, W. Nahaboo, M. Reynders, K. Nekolla, P. Jalinot, J. Hasserodt, M. Rehberg, M. Delattre, S. Zahler, A. Vollmar, D. Trauner and O. Thorn-Seshold, *Cell* **2015**, *162*, 403-411; b) A. J. Engdahl, E. A. Torres, S. E. Lock, T. B. Engdahl, P. S. Mertz and C. N. Streu, *Organic Letters* **2015**, *17*, 4546-4549.
[10] a) W. A. Velema, J. P. van der Berg, M. J. Hansen, W. Szymanski, A. J. M. Driessen and B. L. Feringa, *Nature Chemistry* **2013**, *5*, 924-928; b) M. Wegener, M. J. Hansen, A. J. M. Driessen, W. Szymanski and B. Feringa, *Journal of the American Chemical Society* **2017**, *139*, 17979-17986.
[11] O. Babii, S. Afonin, M. Berditsch, S. Reisser, P. K. Mykhailiuk, V. S. Kubyshkin, T. Steinbrecher, A. S. Ulrich and I. V. Komarov, *Angewandte Chemie-International Edition* **2014**, *53*, 3392-3395.
[12] a) T. Fujino, S. Y. Arzhantsev and T. Tahara, *Journal of Physical Chemistry A* **2001**, *105*, 8123-8129; b) G. S. Kumar and D. C. Neckers, *Chemical Reviews* **1989**, *89*, 1915-1925; c) I. K. Lednev, T. Q. Ye, P. Matousek, M. Towrie, P. Foggi, F. V. R. Neuwahl, S. Umapathy, R. E. Hester and J. N. Moore, *Chemical Physics Letters* **1998**, *290*, 68-74; d) Z. Mahimwalla, K. G. Yager, J. Mamiya, A. Shishido, A. Priimagi and C. J. Barrett, *Polymer Bulletin* **2012**, *69*, 967-1006; e) C. Renner and L. Moroder, *Chembiochem* **2006**, *7*, 869-878.
[13] T. Podewin, M. S. Rampp, I. Turkanovic, K. L. Karaghiosoff, W. Zinth and A. Hoffmann-Roder, *Chemical Communications* **2015**, *51*, 4001-4004.
[14] C. C. Wang, W. C. Lai and W. J. Chuang, *Journal of Biomolecular Nmr* **2014**, *59*, 175-184.
[15] B. Priewisch and K. Ruck-Braun, *Journal of Organic Chemistry* **2005**, *70*, 2350-2352.
[16] W. Freyer, D. Brete, R. Schmidt, C. Gahl, R. Carley and M. Weinelt, *Journal of Photochemistry and Photobiology a-Chemistry* **2009**, *204*, 102-109.
[17] W. Szymanski, J. M. Beierle, H. A. V. Kistemaker, W. A. Velema and B. L. Feringa, *Chemical Reviews* **2013**, *113*, 6114-6178.
[18] E. Ludwig, T. Strunskus, S. Hellmann, A. Nefedov, C. Woll, L. Kipp and K. Rossnagel, *Physical Chemistry Chemical Physics* **2013**, *15*, 20272-20280.
[19] K. H. A. Rosler, J. Wright, K. M. Fox, R. M. Waters and P. S. Callery, *Pharmaceutical Research* **1989**, *6*, 706-708.
[20] S. T. Phillips, M. Rezac, U. Abel, M. Kossenjans and P. A. Bartlett, *Journal of the American Chemical Society* **2002**, *124*, 58-66.
[21] G. N. a. S. Ramachandran, V., *Advances in Protein Chemistry* **1968**, *23*, 283-437.
[22] A. C. Gibbs, L. H. Kondejewski, W. Gronwald, A. M. Nip, R. S. Hodges, B. D. Sykes and D. S. Wishart, *Nature Structural Biology* **1998**, *5*, 284-288.
[23] P. N. Lewis, F. A. Momany and H. A. Scheraga, *Proceedings of the National Academy of Sciences of the United States of America* **1971**, *68*, 2293-&.
[24] M. Berditsch, T. Jager, N. Strempel, T. Schwartz, J. Overhage and A. S. Ulrich, *Antimicrobial Agents and Chemotherapy* **2015**, *59*, 5288-5296.
[25] A. Pantos, I. Tsogas and C. A. Paleos, *Biochimica Et Biophysica Acta-Biomembranes* **2008**, *1778*, 811-823.
[26] A. Desponds and R. Freitag, *Langmuir* **2003**, *19*, 6261-6270.
[27] M. Valiev, E. J. Bylaska, N. Govind, K. Kowalski, T. P. Straatsma, H. J. J. Van Dam, D. Wang, J. Nieplocha, E. Apra, T. L. Windus and W. de Jong, *Computer Physics Communications* **2010**, *181*, 1477-1489.
[28] E. F. Pettersen, T. D. Goddard, C. C. Huang, G. S. Couch, D. M. Greenblatt, E. C. Meng and T. E. Ferrin, *Journal of Computational Chemistry* **2004**, *25*, 1605-1612.

10.1002/cbic.201800618

WILEY-VCH

Entry for the Table of Contents (Please choose one layout)

Layout 1:

FULL PAPER

Gramicidin S mimetic, peptide **2b**, showing a four-fold difference in the minimum inhibitory concentration (MIC) between the *cis*-enriched and *trans*-enriched PSS against *S. aureus*. This photopharmacological approach provides an opportunity to turn antimicrobial activity 'on' and 'off' to allow potential future point-of-care applications.

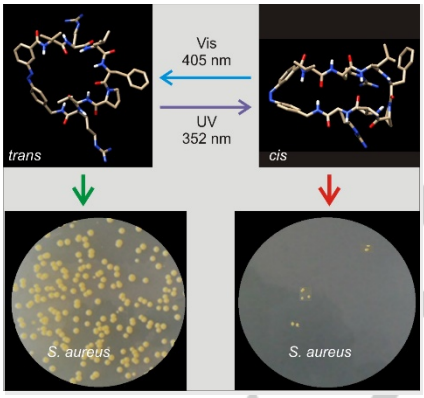

*Yuan Qi Yeoh, Dr. Jingxian Yu, Dr. Steven W. Polyak, Dr. John R. Horsley, Prof. Andrew D. Abell**

Page 1 – Page 6

Photopharmacological Control of Cyclic Antimicrobial Peptides

Layout 2:

FULL PAPER

((Insert TOC Graphic here; max. width: 11.5 cm; max. height: 2.5 cm))

*Author(s), Corresponding Author(s)**

Page No. – Page No.

Title

Text for Table of Contents